Resonance Enhanced Two-Photon Spectroscopy of Magnetically Trapped Atomic Hydrogen

P. W. H. Pinkse, A. Mosk, M. Weidemüller,* M. W. Reynolds, T. W. Hijmans, and J. T. M. Walraven*
Van der Waals–Zeeman Institute, University of Amsterdam, Valckenierstraat 65/67, 1018 XE Amsterdam, The Netherlands

C. Zimmermann
Sektion Physik der Universität München, Schellingstrasse 4/III, 80799 München, Germany
(Received 20 March 1997)

We report on the first results with resonance enhanced two-photon spectroscopy of magnetically trapped atomic hydrogen, exciting the transition from the $1S$ ground state to the $3S$ or the $3D$ state. The spectroscopic method introduces tunable transparency to resonant optical studies of cold dense gases. It combines sensitivity (due to the near resonant $2P$ state) with high resolution (in principle limited only by the $3S$ state lifetime), making it a precision tool for optical investigation of ultracold H gas. To demonstrate its potential, the dynamic evolution of H gas during evaporative cooling is quantitatively investigated by analysis of two-photon absorption spectra. [S0031-9007(97)04129-X]

PACS numbers: 32.80.Pj, 67.65.+z, 32.30.Jc, 32.80.Wr

Hydrogen is the simplest of all elements and its basic properties directly challenge first principle calculations. For instance, the electronic energy levels may be determined theoretically and experimentally with extraordinary high precision, allowing stringent tests of quantum electrodynamics [1]. The recent observation of the $1S$-$2S$ two-photon transition of magnetically trapped H [2] has opened new opportunities for ultraprecise measurements. Optical spectroscopy inside magnetic traps will also find intriguing applications in the future investigations of antihydrogen [3], confined by a magnetic field to prevent annihilation. In the field of ultracold gases atomic H has played a crucial role in the development of trapping and cooling techniques [4,5], notably evaporative cooling, a key element in the recent observation of Bose-Einstein condensation (BEC) in alkali gases [6,7]. Optical diagnostics of atomic H have figured prominently in these studies [8]. In related research, spin-polarized H (confined by liquid helium walls) is studied at high densities as a two or three dimensional quantum gas [9]. Attained densities exceed 10^{13} cm^{-2} in 2D and 10^{19} cm^{-3} in 3D [10]. Here also, optical diagnostics are important.

In this Letter we report on our first results with resonance enhanced two-photon spectroscopy (RETS). These results represent a crucial step towards the application of RETS as a sensitive and accurate diagnostic tool for atomic hydrogen. We excite the transition $1S$-$3S$ or $1S$-$3D$ [see Fig. 1(a)] via the near-resonant intermediate state $2P$ by stacking two copropagating photons, one close to the Lyman-α (121.57 nm) wavelength, and one close to the Balmer-α (656.47 nm) wavelength. This scheme provides high sensitivity due to the resonant enhancement of the transition matrix element by the $2P$ intermediate level. At present the resolution of our method is limited by our Lyman-α source bandwidth (120–150 MHz), but ultimately the resolution is limited only by the lifetime of the $3S$ level ($\tau_{3S} = 160$ ns) and $3D$ level ($\tau_{3D} = 16$ ns), which are much longer than the $2P$ lifetime ($\tau_{2P} = 1.6$ ns). The half-width γ of a line is given by $\gamma = (2\tau)^{-1}$. The small $3S$ linewidth enables determination of the momentum distribution in H gas samples by Doppler spectroscopy down to temperatures below 1 μK, i.e., well below the BEC transition temperature at typical achievable densities (10^{14} cm^{-3}) in traps. In addition, the $1S_{m=1/2}$-$3S_{m=1/2}$ transition shows no first order Zeeman shift, and hence is purely Doppler broadened, greatly facilitating thermometry.

The measurements presented here are performed on magnetically trapped H. We emphasize that the technique itself is of much broader relevance. Future symmetry tests on antihydrogen will most probably start with spectroscopic investigations of a trapped sample with a small number of atoms. Resonance enhanced $1S$-$3S$ spectroscopy offers the perspective of a spectral resolution that is 2 orders of magnitude better than one-photon Lyman-α

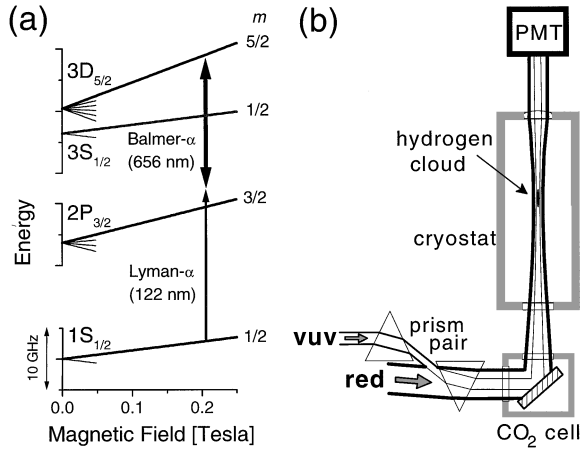

FIG. 1. (a) Relevant energy levels of atomic H as function of magnetic field. (b) Sketch of the experimental setup.

spectroscopy, with, at the same time, a resonant cross section of up to 50% of the $3\lambda^2/2\pi$ single photon Lyman-α cross section.

For high density gases, an important property of RETS is that the absorption cross section for two-photon absorption can be adjusted at will, even on the center of the two-photon resonance, by choosing the detuning from the intermediate $2P$ state. Compared to one-photon spectroscopy, this tunable transparency offers important advantages for the investigation of inhomogeneous dense gases. One may investigate the densest parts of the sample near their resonance frequency without being limited by optical thickness. Resonant imaging of a trapped gas on a two-photon line offers an alternative to the recently demonstrated dark-ground imaging technique [11] for studies of ultracold dense gases. It is clear that for optical investigations on high density samples of spin-down polarized atomic hydrogen (H$\downarrow$), with densities varying between 10^9 and 10^{19} cm^{-3}, tunable transparency may be a key advantage.

The experiments demonstrating RETS of H are performed in a cryogenic Ioffe trap which is described in detail by van Roijen *et al.* [12] and Luiten *et al.* [8]. Pulses (10 ns duration, 1–100 Hz repetition rate) of tunable vacuum-ultraviolet light (VUV) around the Lyman-α wavelength are generated by the system described in [8]. The light is passed through the H gas and is collected by an objective formed by a MgF_2 plano-convex lens at the focal distance of $\sim$15 cm from the sample as shown in Fig. 1(b). The signal-to-noise ratio of the VUV transmission was improved over previous experiments by detecting the VUV beam with a solar-blind photomultiplier (PMT) after passing through the cryostat. Measuring the transmitted intensity at room temperature greatly facilitates detection. Spectral filters may easily be introduced, sensitivity is enhanced, and even spatial analysis of the scattered light becomes possible. Pulse-to-pulse intensity fluctuations were canceled by dividing the measured signal by a reference signal obtained from part of the beam not having passed through the cryostat. Before entering the cryostat, the VUV beam passes through a CO_2 absorption cell to reduce its intensity to a level just above the shot noise limited regime of the final PMT signal. At this intensity sample loss is negligible. Typically 10^7 photons per pulse are focused to a waist of $\sim$180 μm FWHM at the position of the trapped atom cloud, 1 m from the focusing lens, giving a peak intensity of $\sim$4 W cm^{-2}.

The red light near the Balmer-α wavelength is provided by a cw dye laser. With an acousto-optic modulator 200 ns pulses are generated. This light is focused to a waist slightly bigger than that of the VUV, giving an intensity of $\sim 4 \times 10^2$ W cm^{-2}. Chopping the red light between the VUV pulses minimizes thermal load on the cryostat. In addition, delaying every second red pulse so that it does not temporally overlap with the VUV pulse, we measure transmission with and without the red light in the same scan of the VUV frequency. The intense red light is not detected by the solar-blind PMT.

The red beam is spatially overlapped with the VUV beam at one of the monochromator prisms [see Fig. 1(b)]. We verify the overlap by deflecting the two superimposed beams into an evacuated reference system, optimizing the transmission through a 0.3 mm sized pinhole positioned at the same distance from the focusing lens as the sample.

Two-photon transitions to both $3S$ and $3D$ have been observed. Here we focus on the experimental observation of the $3D$ manifold, which contains Zeeman broadened structure and has the advantage of a $10\times$ larger transition matrix element as compared to the $3S$ case.

The important features of RETS for a three-level ladder system are illustrated in Figs. 2(a)–2(d). Plotted is the absolute transmission of the VUV light without any red light [Fig. 2(a)] as a function of the detuning Δ of the VUV from the Lyman-α $1S_{m=1/2}$-$2P_{m=3/2}$ transition frequency at the trap center, and with the red light at three different detunings δ from the Balmer-α $2P_{m=3/2}$-$3D_{m=5/2}$ resonance frequency at the trap center [Figs. 2(b)–2(d)]. Both light beams are σ^+ polarized. The trap was chosen with an offset field $B_0 = 115$ mT in combination with relatively weak radial confinement (31 T m^{-1}), resulting in small angles between the magnetic field and the propagation direction of the light. In this way the nearby $1S_{m=1/2}$-$2P_{m=1/2}$ transition was suppressed to ensure a three-level system. Under our experimental conditions (intense red beam of fixed frequency, weak VUV beam of variable frequency) the method is best described as Lyman-α spectroscopy of H atoms dressed [13] by red light.

In the limit of large δ [Fig. 2(b)], the strong resonance represents the ac Stark-shifted one-photon transition. The weaker resonance at $\Delta \simeq -\delta$ is due to the

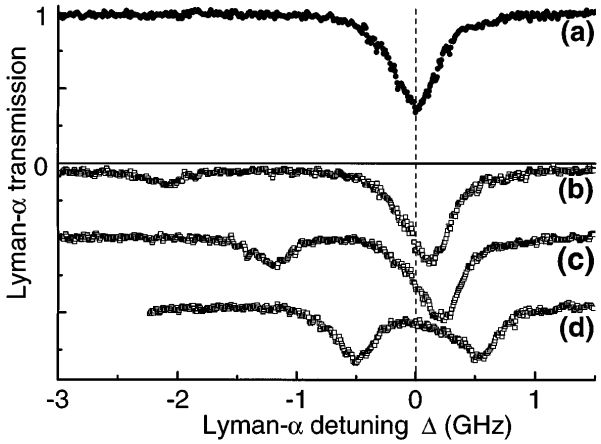

FIG. 2. Lyman-α (122 nm) transmission through a sample of trapped atomic H, without (a) and with (b)–(d) red light of various detunings δ from the Balmer-α (656 nm) transition; (b) $\delta = 2$ GHz; (c) $\delta = 1$ GHz; (d) $\delta = 0$ (Autler-Townes doublet). The 1 GHz splitting is the Rabi frequency $\Omega/2\pi$.

two-photon transition from $1S_{m=1/2}$ to $3D_{m=5/2}$. The corresponding transition probability in this limit scales as $\Omega^2/4\delta^2$, where $\Omega = |\vec{D} \cdot \vec{E}_0|/\hbar$ is the Balmer-α Rabi frequency, with $\vec{E}_0$ the red beam electric field amplitude and $\vec{D} = \langle 3D_{m=5/2}|e\vec{r}|2P_{m=3/2}\rangle$ the transition dipole matrix element from $2P_{m=3/2}$ to $3D_{m=5/2}$. The optical thickness of the sample can therefore be adjusted by simply changing δ while adjusting Δ to maintain the two-photon resonance condition.

In the case $\delta = 0$ the Lyman-α line is split symmetrically into the "Autler-Townes doublet" [14] with peaks at $\Delta_\pm = \pm\Omega/2$ [Fig. 2(d)]. The difference frequency of the two doublet components equals the Rabi frequency of the red beam and thus allows the experimental determination of this important quantity.

The unique combination of high resolution and high sensitivity enables rapid nonperturbative *in situ* studies of the trapped gas. As an example, we observed the evolution of the gas cloud during forced evaporative cooling [4] induced by lowering the field of one of the axial confinement coils. As shown in Fig. 3(a), at a density of 10^{13} cm^{-3} the one-photon spectrum is strongly broadened by optical thickness. The cooling process is monitored by taking spectra at regular time intervals, as shown with the difference spectra of Figs. 3(b)–3(d), for the $1S_{m=1/2}$-$3D_{m=5/2}$ two-photon transition. The resonances shift to lower detunings since the magnetic offset field decreases during the forced evaporation. At the starting conditions, Fig. 3(b), the temperature is 48 mK with the Zeeman broadening dominating over the Doppler effect, yielding the asymmetric two-photon resonance line with a long tail towards higher frequencies. As the sample cools, the cloud shrinks as does the Zeeman broadening, which can be seen from the series of spectra in Figs. 3(b)–3(d). The final spectrum [Fig. 3(d)], at 1 mK, shows a symmetric resonance, its width mainly determined by Doppler broadening and the VUV bandwidth. The ground state hyperfine splitting is clearly resolved.

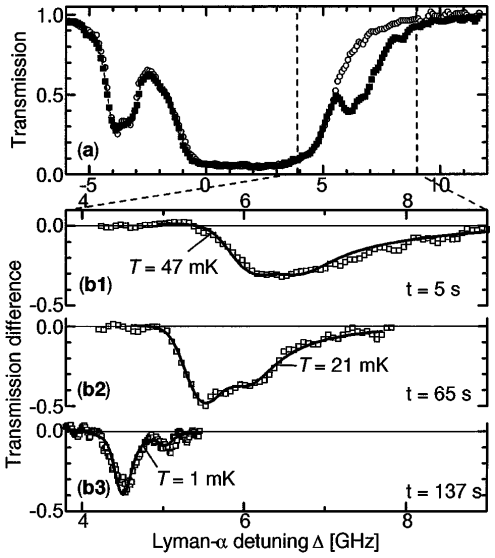

FIG. 3. (a) Lyman-α transmission spectrum without (open circles) and with (solid squares) red light present. $\Delta = 0$ corresponds to the $1S_{m=1/2}$-$2P_{m=3/2}$ transition at the magnetic field minimum. (b1)–(b3) Lyman-α difference spectra (with minus without red light) showing two-photon resonances during forced evaporative cooling of a single sample. Cooling starts at time $t = 0$ in (b1), with central gas density $n = 1.0 \times 10^{13}$ cm^{-3}, number of atoms $N = 1.4 \times 10^{12}$, and temperature $T = 47$ mK, as derived from our fits (solid lines). In (b2) we find $n = 1.0 \times 10^{13}$ cm^{-3}, $N = 2.7 \times 10^{11}$, and $T = 21$ mK, and in (b3) we have $n = 1 \times 10^{13}$ cm^{-3}, $N = 2.6 \times 10^{9}$, and $T = 1$ mK. One scan takes ~5 s.

The number of trapped atoms and the temperature and density of the gas are determined by fitting the observed spectra to calculated curves shown as the solid lines in Figs. 3(b)–3(d). The fitting procedure is based on the following model. Because the red light intensity dominates over the VUV beam intensity, attenuation of the red beam due to two-photon absorption can be neglected. Furthermore, the VUV beam is weak enough that its propagation can be described with an effective susceptibility, proportional to the atomic polarizability α, which depends both upon the local gas properties [8] and the local electric field of the red beam. We use standard resonant scattering theory (see, e.g., [15]) to account properly for the finite lifetimes of the excited states, finding

$$\frac{1}{\alpha} = \frac{1}{\alpha_0} + \frac{\Omega^2/4}{\Delta + \delta + i\gamma_*}, \qquad (1)$$

where $\alpha_0 = 1/(-\Delta - i\gamma_{2P})$ is the polarizability in absence of the red light and γ_* is the half-width of the upper state (γ_{3D} or γ_{3S}). The quantities Δ, δ, and Ω entering the model vary spatially through the nonuniformity of the static magnetic field and the two light beams. The magnetic field is derived from the known geometry of the field coils and the measured currents. The intensity distribution of the red and the VUV light at the position of the atomic sample are determined in the reference system. The Rabi frequency Ω is derived from the measured intensity distribution of the red beam and checked against the splitting of the Autler-Townes doublet. The Doppler broadening is taken into account by introducing a frequency shift in Δ and δ for a moving atom and averaging over a Maxwellian velocity distribution. For comparison with data the calculated spectra are convolved with the spectral profile of the VUV source (Lorentzian, FWHM $\simeq$ 120–150 MHz), estimated from the measured uv spectral profile. Fitting parameters are the density, the temperature, and the relative population of the two trapped hyperfine states. The number of trapped atoms can then be deduced from the density and the temperature taking the known trapping potential into account. Typical accuracies are on the 20 percent level for the absolute values of these quantities, except for the lowest temperatures like Fig. 3(d), where the line shape is strongly influenced by the VUV bandwidth.

Now that we are able to apply and understand RETS in trapped atomic H, many topics are susceptible to investigation even with the present light sources, as we shall discuss at the end of this Letter. RETS becomes much easier once the line width of the VUV source is reduced. A narrowed two-photon peak enhances signal to noise, allowing further detuning and hence less admixture from the broad $2P$ intermediate level. For sufficiently large Δ the three-level system reduces to an effective two-level system and Eq. (1) can be replaced by a simple Lorentzian. Analysis of the spectra should then become particularly simple, especially at low temperatures ($\lesssim$1 mK) where Zeeman broadening can be neglected versus Doppler broadening yielding symmetric line shapes. The resulting line is a convolution of the Gaussian Doppler profile (with a width proportional to the square root of the gas temperature), the natural line profile, and the spectra of the light sources. For possible comparisons between hydrogen and antihydrogen [3], we note that the determination of the relative transition frequency is essentially limited only by the natural line width and the VUV bandwidth.

RETS in principle allows the investigation of the dynamics of H gas with Doppler spectroscopy even in the quantum-statistical regime, directly in velocity space, given a technically feasible bandwidth of 1 MHz for the VUV light source. Optical study of high density samples of H$\downarrow$ atoms, on the other hand, do not require modification of our VUV source. Experiments on H$\downarrow$ are performed at temperatures above 0.1 K; at these temperatures, the lines are Doppler broadened to > 0.6 GHz, much broader than our present VUV source bandwidth. For gas densities exceeding 10^{15} cm^{-3} the average distance between two atoms is less than the wavelength of probe light. In this regime the propagation of light is influenced by quantum correlations in binary radiative collisions [16], but this has not been investigated experimentally, so far. A high density sample of H also offers the possibility of measuring interatomic potentials through the observation of photoassociation lines in the spectrum. Presently, an experiment is being set up in Amsterdam which will allow optical study of a dense gas of H$\downarrow$ in two and three dimensions. For such experiments, RETS is an ideal diagnostic tool.

This work is part of a research program of the Stichting voor Fundamenteel Onderzoek der Materie (FOM), which is a subsidiary of the Nederlandse Organisatie voor Wetenschappelijk Onderzoek (NWO). M. W. acknowledges a HCM/TMR grant from the European Commission. The research of M. W. R. is supported by the Royal Netherlands Academy of Arts and Sciences (KNAW).

*Present address: FOM Institute for Atomic and Molecular Physics (AMOLF), Kruislaan 407, 1098 SJ Amsterdam, The Netherlands.

[1] T. W. Hänsch, in *Atomic Physics*, edited by D. J. Wineland, C. E. Wieman, and S. J. Smith (AIP, New York, 1995), Vol. 14, p. 63, and references therein.
[2] C. L. Cesar, D. G. Fried, T. C. Kilian, A. D. Polcyn, J. C. Sandberg, I. A. Yu, T. J. Greytak, and D. Kleppner, Phys. Rev. Lett. **77**, 255 (1996).
[3] For a review, see M. Charlton, J. Eades, D. Horvath, R. J. Hughes, and C. Zimmermann, Phys. Rep. **241**, 65 (1994).
[4] T. J. Greytak, in *Bose-Einstein Condensation*, edited by A. Griffin, D. W. Snoke, and S. Stringari (Cambridge University Press, Cambridge, 1995), and references therein.
[5] J. T. M. Walraven, in *Quantum Dynamics of Simple Systems*, edited by G. L. Oppo, S. M. Barnett, E. Riis, and M. Wilkinson (Institute of Physics Publishing, Bristol, Philadelphia, 1996).
[6] W. Ketterle and N. J. van Druten, in *Advances in Atomic, Molecular and Optical Physics*, edited by B. Bederson and H. Walther (Academic Press, San Diego, 1996), Vol. 37, p. 181.
[7] M. H. Anderson, J. R. Ensher, M. R. Matthews, C. E. Wieman, and E. A. Cornell, Science **269**, 198 (1995).
[8] O. J. Luiten, H. G. C. Werij, I. D. Setija, M. W. Reynolds, T. W. Hijmans, and J. T. M. Walraven, Phys. Rev. Lett. **70**, 544 (1993).
[9] I. F. Silvera and J. T. M. Walraven, in *Progress in Low Temperature Physics*, edited by D. F. Brewer (Elsevier, Amsterdam, 1986), Vol. 10, p. 139.
[10] E. Tjukanov, A. Ya. Katunin, A. I. Safonov, P. Arvela, M. Karhunen, B. G. Lazarev, G. V. Shlyapnikov, I. I. Lukashevich, and S. Jaakkola, Physica (Amsterdam) **178B**, 129 (1992).
[11] M. R. Andrews, M.-O. Mewes, N. J. van Druten, D. S. Durfee, D. M. Kurn, and W. Ketterle, Science **273**, 84 (1996).
[12] R. van Roijen, J. J. Berkhout, S. Jaakkola, and J. T. M. Walraven, Phys. Rev. Lett. **61**, 931 (1988).
[13] C. Cohen-Tannoudji, J. Dupont-Roc, and G. Grynberg, *Atom-Photon Interactions* (Wiley, New York, 1992).
[14] S. H. Autler and C. H. Townes, Phys. Rev. **100**, 703 (1955).
[15] U. Fano, Phys. Rev. **124**, 1866 (1961).
[16] Yu. Kagan, B. V. Svistunov, and G. V. Shlyapnikov, JETP Lett. **48**, 56 (1988).